

26th International Symposium on Superconductivity, ISS 2013

Trapped field and flux dynamics in MgB_2 superconducting bulks magnetized by pulsed field

H. Fujishiro^{a*}, T. Naito^a, T. Ujiie^a, A. Figini Albisetti^b, G. Giunchi^c

^aDepartment Materials Science and Engineering, Iwate University, Morioka 020-8551, Japan

^bEDISON S.p.A., R&D Division, Foro Buonaparte 31, 20121 Milano, Italy

^cMaterials Science Consultant, via Teodosio 8, 20131 Milano, Italy

Abstract

Pulsed field magnetization (PFM) was performed at $T_s=14$ K for the MgB_2 bulk of 55 mm diameter fabricated by a reactive liquid Mg infiltration (Mg-RLI) method. The time dependence of the local field $B_L^C(t)$ and temperature change $T(t)$ and the trapped field profiles were measured. The numerical simulation of the flux dynamics and heat propagation in the bulk was also performed. The experimental results can be qualitatively explained by the model analyses. We discuss about the characteristic differences of the flux dynamics and heat propagation during PFM between MgB_2 and REBaCuO bulks.

© 2014 The Authors. Published by Elsevier B.V. This is an open access article under the CC BY-NC-ND license (<http://creativecommons.org/licenses/by-nc-nd/3.0/>).

Peer-review under responsibility of the ISS 2013 Program Committee

Keywords: MgB_2 bulk; pulsed field magnetization; trapped field; numerical simulation

1. Introduction

MgB_2 bulk magnet has attractive features such as low cost, light-weight, and weak-link-free homogeneous current flow, which are a clear contrast with REBaCuO superconducting bulk magnets (RE=rare earth element). To magnetize the REBaCuO bulks, a field-cooled magnetization (FCM) is used usually. A pulsed field magnetization (PFM) has been recently investigated because of an inexpensive and mobile experimental set-up with no need of a superconducting magnet. However, the trapped field B_z achievable by PFM is nonetheless lower than that achievable by FCM because of a large temperature rise caused by the dynamical motion of the magnetic flux. We have investigated the PFM procedure experimentally and numerically for the REBaCuO bulks to enhance the trapped field [1]. On the other hand, for MgB_2 bulks, the results of the trapped field by FCM have been mainly reported; the

* Corresponding author. Tel.: +81-19-621-6363; fax: +81-19-621-6363.

E-mail address: fujishiro@iwate-u.ac.jp

maximum trapped field was 2.25 T at 15 K on the single MgB₂ bulk [2] and 3.14 T at 17.4 K in the bulk pair [3]. We have performed the PFM procedure for the MgB₂ bulks fabricated by various methods [4, 5], where the maximum trapped field was as low as 0.71 T at 16 K for the bulk fabricated by a capsule method [4].

To enhance the trapped field on the MgB₂ bulk by PFM, we must consider the inherent nature of the MgB₂ bulk. That is, the thermal properties such as thermal conductivity $\kappa(T)$ and specific heat $C(T)$ and the magnetic field dependence of the critical current density $J_c(B)$ are fairly different from those of REBaCuO bulk at operating temperature. In this study, we performed the PFM experiments for the MgB₂ bulk fabricated by a reactive liquid Mg infiltration (Mg-RLI) [6], which can realize a large and homogeneous MgB₂ bulk. A numerical simulation was also performed considering the flux dynamics and heat conduction in the bulk. The magnetic flux intrusion and flux trapping during PFM are discussed, compared with those for the REBaCuO bulk.

2. Experimental procedure

The MgB₂ bulk disk of 55 mm in diameter and 15 mm in thickness was prepared, which was fabricated by the Mg-RLI technique [6]. The superconducting transition temperature T_c and the trapped field B_z at 20 K by FCM were, respectively, confirmed to be 38 K and 1.40 T. Figure 1 shows the experimental setup for PFM around the bulk and the magnetizing pulse coil. The bulk, mounted in stainless steel (SUS316L) rings of 8 mm thickness, was tightly anchored onto the cold stage of a Gifford–McMahon (GM) cycle helium refrigerator. The initial temperature T_s of the bulk was set to 14 K. A magnetizing solenoid coil (94 mm i.d., 153 mm o.d., and 50 mm height), which was dipped in liquid nitrogen, was placed outside the vacuum chamber. A magnetic pulse $B_{ex}(t)$ with a rise time of 0.013 s and a duration time of 0.15 s was applied to the bulk by flowing the pulsed current from a condenser bank. The time evolutions of the local field $B_L^C(t)$ and the subsequent trapped field B_z at the center of the bulk surface ($z=0$ mm) were monitored by Hall sensors (F W Bell, BHA 921) using a digital oscilloscope. Two-dimensional trapped field profiles of B_z ($z=1$ mm) were mapped at a distance of 1 mm above the bulk surface.

3. Modeling and numerical simulation

Based on the experimental setup shown in Fig. 1, the framework of the numerical simulation was constructed. Physical phenomena during PFM were described using electromagnetic and thermal equations. The details of the simulation are described elsewhere [7]. The power- n model ($n=100$) was supposed to describe the nonlinear E - J characteristic in the bulk. The magnetic field dependence of the critical current density $J_c(B)$ for the Mg-RLI bulk was fitted using the equation of $J_c(B)=J_{c0}\exp[-(B/B_0)^{1.5}]$ ($B_0=1.25$) based on the previous report [8], where J_{c0} ($=2.2 \times 10^9$ A/m² at 14 K) is the critical current density under zero field. The temperature dependences of the specific heat $C(T)$ and the thermal conductivity $\kappa(T)$ for the present MgB₂ bulk [9, 10] and SUS ring were also introduced in the numerical simulation.

4. Results and discussion

4.1. Experimental results

Figure 2 shows the trapped field B_z at the center of the bulk surface, as a function of the applied pulsed field B_{ex} . B_z increases for $B_{ex}>1$ T, takes a maximum at $B_{ex}=1.79$ T and then decreases with increasing B_{ex} . The maximum B_z was 0.41 T. The B_z vs B_{ex} curve and the maximum B_z are typical for PFM of MgB₂ bulks [5, 6].

Figures 3(a) and 3(b) present the trapped field profiles $B_z(z=1$ mm) on the bulk for $B_{ex}=1.17$ T and 1.79 T and Figure 3(c) shows the cross sections of the B_z profiles along $x=0$ mm. For $B_{ex}=1.17$ T, the magnetic flux was trapped only at the bulk periphery, which comes from the strong inner shielding current. For $B_{ex}=1.79$ T, the magnetic flux intrudes into the center and the trapped field profile is nearly the conical one. The conical B_z profile maintains for $B_{ex}>1.97$ T with the decrease in the maximum value. Figure 4 shows the time evolution of the applied field $B_{ex}(t)$ and local field $B_L^C(t)$ at the center of the bulk surface for typical applied field. For each B_{ex} , $B_L^C(t)$ starts to increase for $t=0.005$ s with a time delay, takes a maximum at 0.02 s, and then decreases to a final value due to the flux flow.

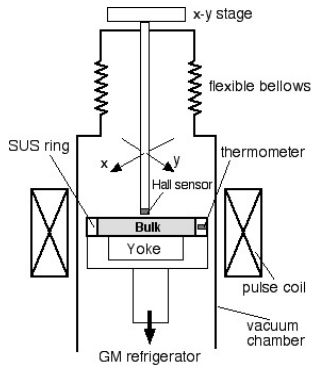


Fig. 1. Experimental PFM setup around the bulk and applied magnetizing coil.

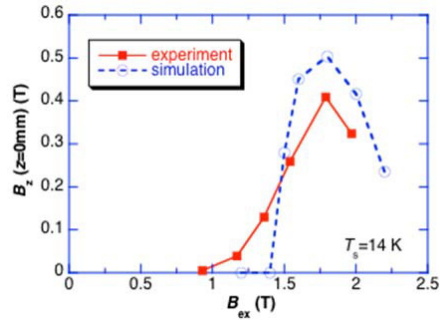


Fig. 2. Trapped field B_z ($z=0\text{mm}$) at $T_s=14\text{ K}$ on the bulk as a function of the pulsed field B_{ex} . The result of the simulation is also shown.

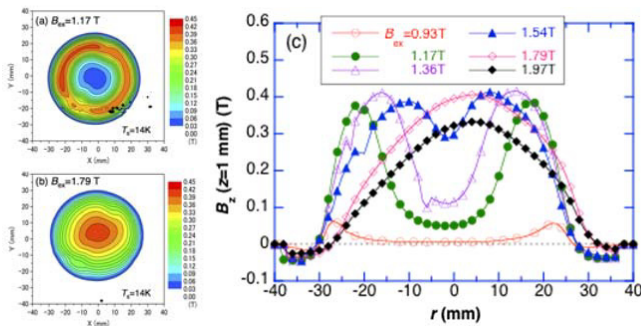


Fig. 3. Trapped field profiles at $z=1\text{ mm}$ above the bulk surface for (a) $B_{ex}=1.17\text{ T}$ and (b) 1.79 T . (c) Cross sections of the trapped field profiles at $z=1\text{ mm}$.

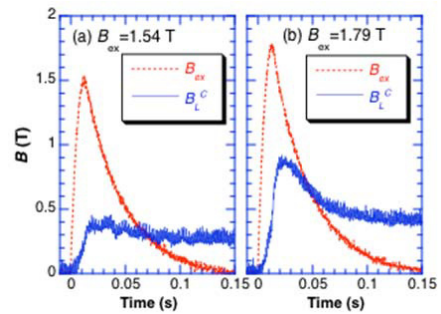


Fig. 4. Time evolution of the applied field $B_{ex}(t)$ and local field $B_L^C(t)$ for (a) $B_{ex}=1.54\text{ T}$ and (b) 1.79 T .

4.2. Results of numerical simulation and discussion

The result of the simulation for the trapped field B_z at the centre of the bulk surface as a function of applied pulsed field was shown in Fig. 2. The B_z vs B_{ex} behaviour reproduces the experimental one qualitatively. The difference of the maximum B_z value may come from the difference of J_{c0} and/or $J_c(B)$ characteristics. Figure 5 shows the results of the simulation of the cross sections of the trapped field profile B_z for typical B_{ex} values. The profile changes from concave to convex (or flat) with increasing B_{ex} and then the maximum B_z decreases, which reproduces the experimental results qualitatively as shown in Fig. 3.

Figure 6 presents the results of the simulation of the time dependence of the local field $B_L^C(t)$ at $r=0, 10$ and 20 mm for $B_{ex}=1.5\text{ T}$ and 1.8 T . The magnetic flux intrudes from the bulk periphery and B_L^C at the bulk centre ($r=0\text{ mm}$) starts to rise with a slight time delay. The similar time delay can be observed in the experiments shown in Fig. 4, but in the simulation, the time delay is larger, compared with the experiments.

Finally, we discuss about the difference the flux dynamics during PFM between MgB_2 and REBaCuO bulk. First, we must comment on the specific heat C per unit volume and thermal conductivity κ for both bulk systems. At the typical operating temperature, for example, $T_s=14\text{ K}$ for MgB_2 and $T_s=40\text{ K}$ for REBaCuO , the specific heat per unit volume of MgB_2 is $2 \times 10^{-4}\text{ J/cm}^3\text{K}$ [9], which is three-orders of magnitude smaller than that for GdBaCuO at 40 K . In addition, the thermal conductivity of MgB_2 is 40 W/mK at 14 K [10], which is about three times larger, compared with that of the GdBaCuO bulk at 40 K . The difference of these thermal properties between two systems may seriously influence on the flux dynamics and heat propagation. Second, $J_c(B)$ characteristics are quite different; the $J_c(B)$ characteristics of the REBaCuO bulk show the well-known peak effect and the irreversibility field B_{irr} was

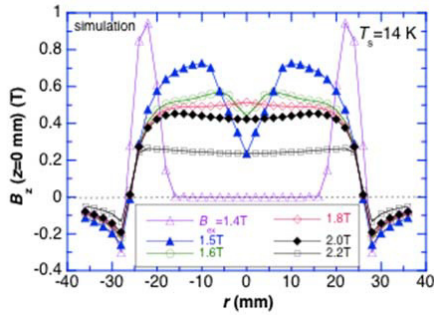


Fig. 5. Cross sections of the trapped field profile B_z for typical B_{ex} values. (simulation)

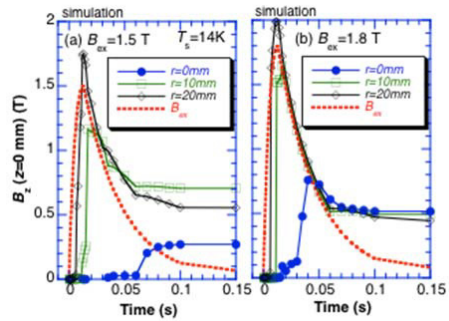


Fig. 6. Time dependence of the local field $B_L^C(t)$ at $r=0, 10$ and 20 mm for $B_{ex}=1.5$ T and 1.8 T at 14 K. (simulation)

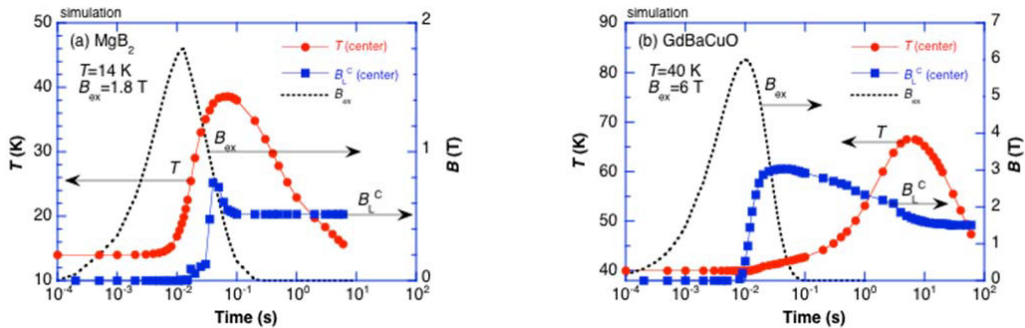


Fig. 7. Time dependence of the local field B_L^C and temperature T (a) for the MgB_2 bulk after applying the pulsed field of 1.8 T at 14 K and (b) for the $GdBaCuO$ bulk after applying the pulsed field of 6.0 T at 40 K [8]. (simulation)

enhanced. On the other hand, $J_c(B)$ of MgB_2 monotonically decreases with increasing applied field. The temperature margin between T_s and T_c for the MgB_2 is smaller than that for the $REBaCuO$, which may also affect the stability.

Figure 7(a) shows the results of the simulation of the time dependence of the local field B_L^C and temperature T after applying the pulsed field of 1.8 T at 14 K. For comparison, the similar results of the simulation were also shown in Fig. 7(b), where the pulsed field of 6 T was applied for the $GdBaCuO$ bulk at 40 K [7]. It should be noticed that the flux creep terminates in 0.1 s and the temperature rise recovered within 10 s for the MgB_2 system, mainly because of small $C(T)$, large $\kappa(T)$ and poor $J_c(B)$ characteristics. On the other hand, for the $GdBaCuO$ system, the flux creep continues and terminates in about 10 s because the temperature rise recovered in about 100 s.

In summary, time dependence of the local field $B_L^C(t)$ and temperature change $T(t)$ and the trapped field profiles of the MgB_2 bulk during PFM can be qualitatively explained by the model analyses. The flux dynamics and heat generation in the MgB_2 bulk are clear contrast with those in the $REBaCuO$ bulks.

References

- [1] H. Fujishiro, T. Tateiwa, A. Fujiwara, T. Oka, H. Hayashi, *Physica C*, **445–448** (2006) 334.
- [2] A. Yamamoto, H. Yumoto, J. Shimoyama, K. Kishio, A. Ishihara, M. Tomita, *Proc. Abstract 23rd Int. Symp. Supercond.*, (2010) 219.
- [3] J.H. Durrell et al., *Supercond. Sci. Technol.* **25** (2012) 112002.
- [4] H. Fujishiro, T. Naito, T. Sasaki, T. Arayashiki, *Proc. ICEC24-ICMC2012* (2013) 571.
- [5] H. Fujishiro, T. Tamura, T. Arayashiki, M. Oyama, T. Sasaki, T. Naito, G. Giunchi, A. Albisetti, *Jpn. J. Appl. Phys.* **51** (2012) 103005
- [6] G. Giunchi, S. Ceresara, G. Ripamonti, S. Chiarelli, M. Spadoni, *IEEE Trans. Appl. Supercond.* **13** (2003) 3060.
- [7] H. Fujishiro, T. Naito, *Supercond. Sci. Technol.* **23** (2010) 105021.
- [8] F.X. Xiang, X.L. Wang, X. Xun, K.S.B. De Silva, Y.X. Wang, S.X. Dou, *Appl. Phys. Lett.* **102** (2013) 152601.
- [9] Y. Wang, T. Plackowski, A. Junod, *Physica C* **355** (2001) 179.
- [10] T. Cavallin, E.A. Young, C. Beduz, Y. Yang, G. Giunchi, *IEEE Trans. Appl. Supercond.* **17** (2007) 2770.